Check for updates

Received: 22 December 2020 | Revised: 3 May 2021 | Accepted: 5 May 2021

DOI: 10.1002/hyp.14210

RESEARCH ARTICLE

WILEY

Storage-discharge characteristics of an active rock glacier catchment in the Innere Ölgrube, Austrian Alps

Thomas Wagner[1,3] | Simon Kainz[1] | Karl Krainer[2] | Gerfried Winkler[1]

[1]Institute of Earth Sciences, NAWI Graz Geocenter, University of Graz, Graz, Austria

[2]Institute of Geology, University of Innsbruck, Innsbruck, Austria

[3]Geo5 GmbH, Roseggerstraße 17, 8700, Leoben, Austria

Correspondence
Thomas Wagner, Institute of Earth Sciences, NAWI Graz Geocenter, University of Graz, Heinrichstrasse 26, 8010 Graz, Austria.
Email: thomas.wagner@uni-graz.at.

Funding information
Austrian Federal Ministry of Agriculture, Regions and Tourism, Grant/Award Numbers: RG-AlpCatch (Nr. 101561), RGHeavyMetal (Nr. 101093); Federal State of Tyrol, Grant/Award Numbers: RG-AlpCatch (Nr. 101561), RGHeavyMetal (Nr. 101093); Federal State of Carinthia, Grant/Award Numbers: RG-AlpCatch (Nr. 101561), RGHeavyMetal (Nr. 101093); Federal State of Styria, Grant/Award Numbers: RG-AlpCatch (Nr. 101561), RGHeavyMetal (Nr. 101093); Federal State of Vorarlberg, Grant/Award Numbers: RG-AlpCatch (Nr. 101561), RGHeavyMetal (Nr. 101093); Federal State of Salzburg, Grant/Award Numbers: RG-AlpCatch (Nr. 101561), RGHeavyMetal (Nr. 101093)

Abstract

The active rock glacier "Innere Ölgrube" and its catchment area (Ötztal Alps, Austria) are assessed using various hydro(geo)logical tools to provide a thorough catchment characterization and to quantify temporal variations in recharge and discharge components. During the period from June 2014 to July 2018, an average contribution derived from snowmelt, ice melt and rainfall of 35.8%, 27.6% and 36.6%, respectively, is modelled for the catchment using a rainfall-runoff model. Discharge components of the rock glacier springs are distinguished using isotopic data as well as other natural and artificial tracer data, when considering the potential sources rainfall, snowmelt, ice melt and longer stored groundwater. Seasonal as well as diurnal variations in runoff are quantified and the importance of shallow groundwater within this rock glacier-influenced catchment is emphasized. Water derived from ice melt is suggested to be provided mainly by melting of two small cirque glaciers within the catchment and subordinately by melting of permafrost ice of the rock glacier. The active rock glacier is characterized by a layered internal structure with an unfrozen base layer responsible for groundwater storage and retarded runoff, a main permafrost body contributing little to the discharge (at the moment) by permafrost thaw and an active layer responsible for fast lateral flow on top of the permafrost body. Snowmelt contributes at least 1/3rd of the annual recharge. During droughts, meltwater derived from two cirque glaciers provides runoff with diurnal runoff variations; however, this discharge pattern will change as these cirque glaciers will ultimately disappear in the future. The storage-discharge characteristics of the investigated active rock glacier catchment are an example of a shallow groundwater aquifer in alpine catchments that ought to be considered when analysing (future) river runoff characteristics in alpine catchments as these provide retarded runoff during periods with little or no recharge.

KEYWORDS
Austrian Alps, catchment characterization, isotopes, permafrost, rainfall-runoff modelling, rock glacier

This is an open access article under the terms of the Creative Commons Attribution-NonCommercial License, which permits use, distribution and reproduction in any medium, provided the original work is properly cited and is not used for commercial purposes.
© 2021 The Authors. *Hydrological Processes* published by John Wiley & Sons Ltd.

1 | INTRODUCTION

Rock glaciers, moraines and talus slopes as the most important alpine coarse-grained sediment deposits may play a critical role in providing groundwater discharge in alpine catchments (besides highly fractured or karstified bedrock aquifers) that sustain baseflow in larger river systems further downstream (Hayashi, 2020). Intact, particularly active rock glaciers on the one hand may store hydrologically valuable ice volumes (Jones et al., 2018) and on the other hand act as shallow groundwater storages or reservoirs in alpine headwaters (Jones et al., 2019; Wagner, Brodacz, et al., 2020; Winkler et al., 2016, 2018). To fully recognize the hydrological cycle in alpine regions, shallow groundwater systems such as rock glaciers need to be better understood in the light of climate change as these water storages/buffers are expected to be more resilient than, for example ice glaciers (Jones et al., 2019; Wagner, Kainz, et al., 2019; Wagner, Pauritsch, et al., 2019). In the last decades, investigations related to the hydro(geo)logy of rock glaciers were thus intensified (e.g., Harrington et al., 2018; Hayashi, 2020; Krainer et al., 2007; Krainer & Mostler, 2002; Winkler et al., 2016) and further research is warranted.

Rock glaciers evolve from active, downslope creeping rock-ice mixtures to inactive (still containing permafrost ice, but not moving anymore) and further to relict, permafrost ice-free, distinct debris accumulations (e.g., Barsch, 1996; Berthling, 2011)). Relict rock glaciers display a complex internal structure (e.g., Zurawek, 2002) and can be characterized as aquifers with at least a fast and a delayed flow component (Pauritsch et al., 2015, 2017; Winkler et al., 2016). The delayed flow component is related to a fine-grained base layer representing the main shallow groundwater component, whereas lateral flow in the coarser upper layers allows generating a fast-flow component.

Geophysical investigations and drillings showed that intact, permafrost ice containing rock glaciers have an unfrozen base layer underneath the permafrost ice-debris main body that is up to more than 10 m thick and contains high amounts of fine-grained sediment (Hausmann et al., 2007, 2012; Krainer et al., 2015). This unfrozen base layer is interpreted to be responsible for base flow during longer periods of little to no recharge (e.g., winter; Wagner, Brodacz, et al., 2020). Lateral flow on top of the permafrost body (within the active layer; e.g., Krainer et al., 2007; Winkler et al., 2018) or along channels within the permafrost body (related to talik formation; e.g., Arenson et al., 2010; Zenklusen Mutter & Phillips, 2012) might be responsible for a fast-flow component. The actual contribution of potential permafrost ice melt is another component that needs further attention (besides increasing storage capacity due to melting of ice; cf. Rogger et al., 2017). In addition, cirque glaciers or remnants thereof in the upper catchment of a rock glacier provide recharge/meltwater which may affect the flow dynamics of rock glacier springs and act as an additional runoff component (e.g., Wagner, Brodacz, et al., 2020) that might decrease as climate warming continues (Shannon et al., 2019).

The aim of this study is to (i) differentiate between various sources of recharge (namely rainfall, snowmelt and ice melt from cirque glaciers within the rock glacier catchment) and (ii) quantify the diurnal and seasonal patterns of the individual contributions in addition to delayed groundwater to the discharge at the rock glacier springs. (iii) The ice melt contribution (from permafrost and cirque glaciers) to spring discharge is discussed in the light of climate change and uncertainties of the methods applied. The quantification of individual flow and recharge components in such a setting has not been done before and is considered as an important step towards a better understanding of climate change impact in alpine catchments.

2 | STUDY AREA

The Innere Ölgrube rock glacier (also known as Ölgrube Süd; "inner" or "southern" as the valley head is towards south) is an active rock glacier located about 1.5 km southeast of the Gepatsch hut in a small, west-facing tributary valley of the Kauner Valley in the western Ötztal Alps of North Tyrol (Austria) at an average elevation of 2582 m a.s.l. with an areal extent of ~0.24 km^2 (Figure 1). The rock glacier catchment area measures ~1.83 km^2 and the bedrock as well as the moraine and talus deposits consist of orthogneiss, paragneiss and mica schists of the Ötztal-Stubai Metamorphic Complex (Hoinkes & Thöni, 1993). Two small cirque glaciers ("western Hintere Ölgruben Ferner" and "Hintere Ölgruben Ferner") covering an area of ~0.16 km^2 are (still) present within the catchment (Buckel & Otto, 2018). A small creek evolving from glacier meltwater infiltrates a few 10 of meters downstream of the lower glacier. Another (very likely the same) creek appears further down below a moraine ridge, which infiltrates at the rooting zone of the rock glacier. The rock glacier is composed of two tongue-shaped lobes with a length of 896 m and a width of 334 m; the northern, larger lobe is composed of orthogneiss debris, the smaller southern lobe of paragneiss and mica schists. Transverse and longitudinal furrows and ridges characterize the distinct surface morphology. The rooting zone is at an elevation of 2727 m and the active front that is up to 70 m high with a steep gradient of 40–45° is located at an elevation of 2394 m (Berger et al., 2004).

At the base of the steep front several springs are developed (Figure 1(c); details see Berger et al., 2004; Hausmann et al., 2012; Krainer & Mostler, 2002, 2006; Krainer et al., 2007). The rock glacier is active. During the period 2002–2005 flow velocities of up to 2.5 m/year were recorded near the front (Krainer & Mostler, 2006). A more recent analysis of Groh and Blöthe (2019) based on image tracking is consistent with these observations, indicating a maximum of 1.7 m/year for the period 2003–2015. The internal structure of the rock glacier was determined by geophysical methods (ground penetrating radar, seismics, and gravimetry; Hausmann et al., 2012). The rock glacier is composed of an active layer with a thickness of 4–6 m which is underlain by the permafrost body (20–30 m). Ice-content in the permafrost body ranges from 40% to 60% (Hausmann et al., 2012). Between the permafrost body and the bedrock an ice-free sediment layer is present, which is 10–15 m thick. This unfrozen sediment layer is interpreted to represent a shallow groundwater

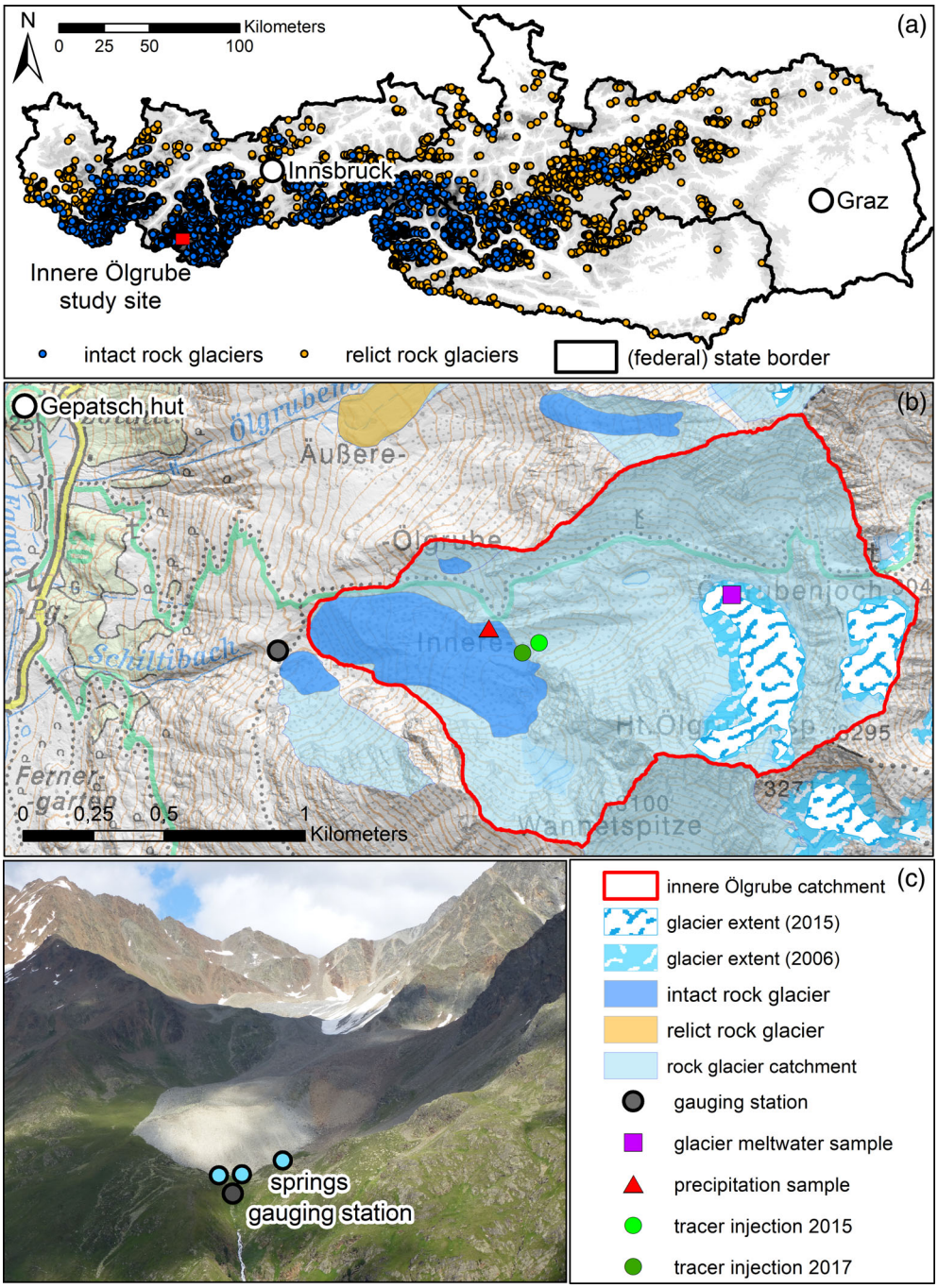

FIGURE 1 Innere Ölgrube rock glacier and its catchment area. (a) Location of Innere Ölgrube within Austria relative to all 5769 rock glaciers mapped in the Austrian Alps (Wagner, Pleschberger, et al. 2020; Wagner, Ribis, et al. 2020). (b) Topographic map of the Innere Ölgrube rock glacier and its catchment (red polygon) including the extents of two cirque glaciers for the years 2006 and 2015. Location of the gauging station, of the precipitation and the glacier meltwater samples and the two artificial tracer injection points are depicted. Rock glacier and catchment extents from Wagner, Pleschberger, et al. (2020), Wagner, Ribis, et al. (2020); glacier extents from the Austrian glacier inventories GI3 (Fischer et al., 2015) and GI4 (Buckel & Otto, 2018). (c) Field impression of the two tongues of the active Innere Ölgrube rock glacier seen from the western side of the Kauner valley viewing towards east. Note the active (unweathered) steep slope of the fronts; the creek ("Schiltibach") which emerges below is the result of several springs at the base of the rock glacier front

storage responsible for base flow even during winter (Wagner, Brodacz, et al., 2020).

3 | DATA AND METHODS

3.1 | Spring hydrograph

Spring discharge data for the time period June 2014 to June 2017 was analysed among other discharge data from active rock glacier springs by Wagner, Brodacz, et al. (2020) using master recession curves based on the approach proposed by Posavec et al. (2017). Fitted recession functions are based on the exponential model of Maillet (1905) and related assumptions are described in more detail in Wagner, Brodacz, et al. (2020). The recession coefficients are shown simply to note that the more recently available discharge data did not change the master recession curves as used in Wagner, Brodacz, et al. (2020) and therefore their conclusions are still valid.

Here we use the same spring discharge data from Wagner, Brodacz, et al. (2020) and add more recent data until July 2018 to overlap with available natural tracer data (Figure 2). On the one hand, the discharge time series data are used to calibrate and validate the rainfall-runoff model, but the recession coeffcients of the master recession curve are not considered in the rainfall-runoff model (see

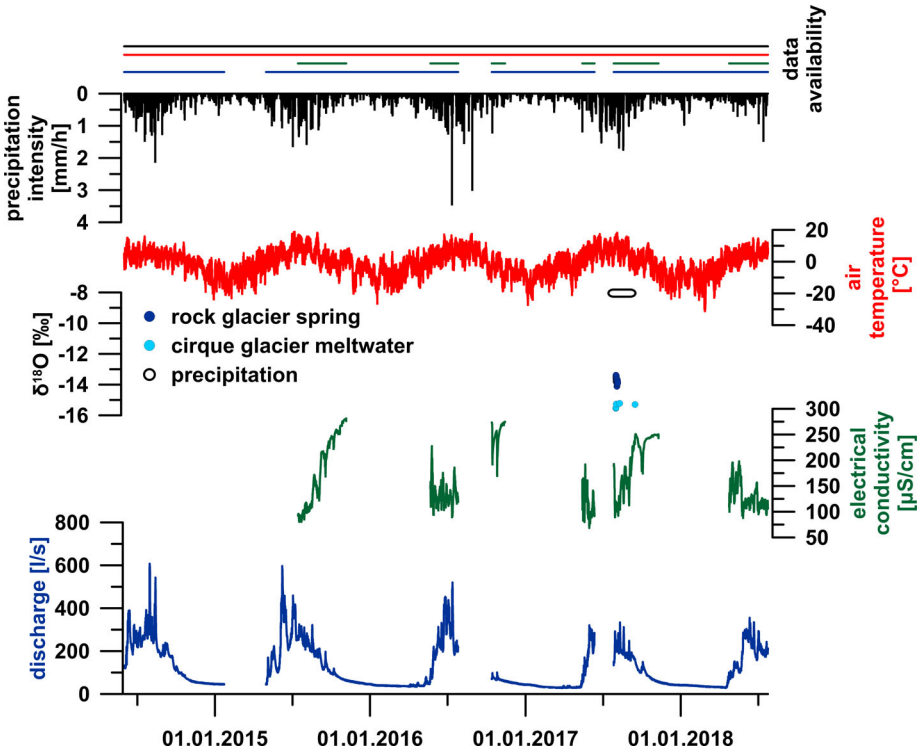

FIGURE 2 Data overview. Precipitation and air temperature data (from the Weißsee station [TIWAG] and corrected to the average elevation of the catchment), isotopic data sampled at the gauging station as well as within the spring catchment, EC and discharge from the gauging station

Section 3.3). On the other hand, the data serve as a base for a detailed flow component separation in combination with electrical conductivity (EC) and isotopic data.

Water level and EC were measured directly at the gauging station (Figure 1(b)). The former was converted to discharge by applying a rating curve based on the salt dilution method implemented under a wide range of flow conditions (Heigert, 2018). Several data gaps in the discharge and EC record are due to the harsh alpine environment and related maintenance restrictions (Figure 2). However, the overall dynamics are captured reasonably well and the presented analyses take the associated uncertainties into account. Note that in contrast to the pressure probe, the EC probe fell dry due to low water levels during the winter months as the probe is situated higher than the pressure probe (Figure 2). Precipitation and air temperature were recorded at a measurement interval of 15 min at the meteorological station Weißsee (2464 m a.s.l.; distance ~4 km to the southwest; courtesy of TIWAG). The mean catchment air temperature and precipitation were calculated applying a correction factor of 0.5°C/100 m and 7% / 100 m, respectively, to account for the mean catchment elevation of 2887 m a.s.l. (Kuhn et al., 2013; Wagner, Brodacz, et al., 2020).

3.2 | Tracers analysis

3.2.1 | Artificial tracers

Artificial tracers were applied to infer the connection between glacier input from the meltwater stream and the rock glacier spring. Tracer injection was downstream of the cirque glaciers where the glacier meltwater infiltrates into the sediments in the vicinity of the rooting zone of the rock glacier (which is already disconnected from the cirque glaciers; Figure 1(b)). Two tracer experiments were performed with injection points along the creek that infiltrates into the rooting zone of the rock glacier in two different years (Figure 1(b); 2015: distance to the gauging station ~980 m; 2017: distance to the gauging station ~910 m) using fluorescein as a conservative dye tracer. In 2015, 25 g of tracer were injected, in 2017 a greater amount of 202.5 g was used. Detection of tracer concentrations was done using a field fluorometer GGUN-FL30 (Abilla Co.; Schnegg, 2002) installed at the gauging station. Linear flow velocities were calculated based on the observed peak tracer concentration as well as on the mean tracer residence time using the method of moments (Kreft & Zuber, 1978).

3.2.2 | Natural tracers

Time series of EC available at the gauging station were used in combination with individual samples analysed for EC and stable isotopes ($\delta^{18}O$ and $\delta^{2}H$) taken during various field trips between 31 July 2017 and 15 September 2017. These samples include glacial meltwater (four samples), a cumulative rainfall sample collected during the same period using a funnel connected via a flexible tube to a bottle (placed 1 m deep within the coarse blocky surface to avoid evaporation by direct radiation), as well as 18 samples taken by an automatic sampler between 01 August 2017 and 06 August 2017 (Figure 2; sampling locations indicated in Figure 1(b)). During field campaigns no direct access to permafrost ice (below the active layer) was obtained, so the

actual signature of permafrost ice in this catchment remains unknown.

Natural tracer data (EC, isotopes) allow to determine variations in fast-flow components of groundwater from the endmembers of rainfall, snowmelt and ice melt (e.g., Winkler et al., 2016). The restricted rock-water interaction in the alpine catchment composed of metamorphic bedrock allows regarding EC as a conservative tracer (cf. Winkler et al., 2016). Water passing quickly through the aquifer can be recognized by low EC values. Based on this assumption a two-component mixing model was applied to identify delayed and fast groundwater flow components (hereafter delayed flow and fast-flow) at diurnal and seasonal time scales (Harrington et al., 2018; Williams et al., 2006; Winkler et al., 2016). The fast-flow component is composed of low mineralized rainfall, snowmelt and / or glacier ice melt, which is distinguishable from the higher mineralized delayed flow component. The actual fast-flow component (i.e., rainfall, snowmelt or ice melt) is derived from EC and isotopic analysis.

3.3 | Rainfall-runoff modelling

For a better understanding of the discharge pattern and to further constrain the contribution of rainfall, snowmelt and ice melt within the rock glacier catchment, a parsimonious lumped parameter rainfall-runoff model was deployed.

The model is based on the simple rainfall-runoff model GR4J of Perrin et al. (2003) using a daily time step and a uniform spatial distribution of precipitation. It was successfully extended and applied for a relict rock glacier and catchments downstream of relict rock glaciers by Wagner et al. (2016) using a snow module based on Majone et al. (2010) and potential evapotranspiration is computed according to Oudin et al. (2005). This model was shown to be especially valuable in alpine catchments where input data are usually scarce (e.g., Wagner et al., 2013, 2016) and also where discharge fluctuates heavily as for karst systems (e.g., Kaminsky et al., 2021; Wagner et al., 2013) and therefore catchment hydrologic response is likely to be assured (cf. Basso et al., 2015).

The model has seven parameters that are free to be calibrated (Figure 3; the symbols are kept as introduced by Perrin et al. (2003) and Wagner et al. (2016) for comparability): ×1 (the maximum capacity of the production or soil moisture accounting store in mm); ×2 (a water exchange coefficient in units of mm that can be positive if water enters the catchment, negative if water exits the catchment unobserved, or zero if there is no water exchange); ×3 (the maximum capacity of the routing store in mm); ×4 (a time parameter expressed in units of days) and the temperature dependent parameters of the snow module: Ts (temperature at which snow starts to fall); Tm (temperature at which snow starts to melt); and Cm (melt factor that allows a certain amount of snowmelt per degree temperature increase). The time parameter ×4 is applied for the unit hydrographs UH1 and UH2 that are used to simulate the time lag between a rainfall event and the resulting stream flow. For UH1 the water is distributed over a number of days (smallest integer exceeding ×4) with its maximum at the last day of the hydrograph. For UH2 the water is distributed over a time period about twice the number of days of UH1 (smallest integer exceeding 2 * ×4). The peak outflow is reached at a similar time as the peak for UH1, then the water outflow decreases to zero at the end.

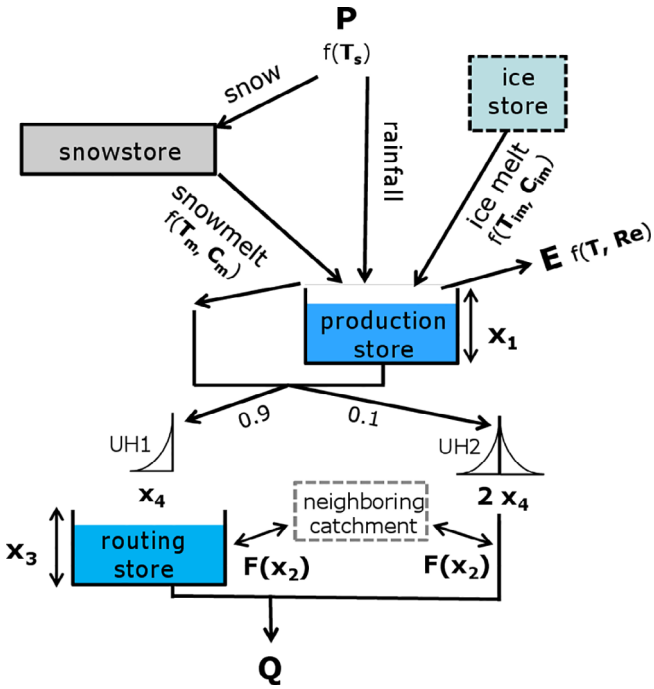

FIGURE 3 Model structure of the rainfall-runoff model GR4J+ with a daily time step and an additional ice store (modified after Wagner et al., 2016). P = precipitation; T = air temperature; Ts = temperature at which snow starts to fall; Tm = temperature at which snow starts to melt; Cm = melt factor that allows a certain amount of snowmelt per degree temperature increase; Tim = temperature at which ice starts to melt (if snow is absent); Cim = melt factor that allows a certain amount of ice melt per degree temperature increase; Re = extraterrestrial solar radiation; ×1 = maximum capacity of the production store; E = actual evapotranspiration; F = groundwater exchange term acting on the fast and slow flow components; ×2 = water exchange coefficient; ×3 = maximum capacity of the routing store; ×4 = time parameter; UH1 and UH2 = unit hydrographs to account for the time lag between rainfall and resulting streamflow that depend on the time parameter ×4; Q = runoff simulated by the rainfall-runoff model

Here, the model was extended by an ice store module (Figure 3) to account for ice melt within the spring catchment. The module is based on a degree-day factor and contributes ice melt as input in the production store if seasonal snow is melted as described in Nepal et al. (2017). The two additional model parameters that are free to be calibrated are Tim (temperature at which ice starts to melt if snow is absent) and Cim (melt factor that allows a certain amount of ice melt per degree temperature increase). This model setup relates ice melt to melt from glaciers and not from permafrost. For simplicity the initial glacier ice water volume is assumed to be large so that over the analysed period of more than 4 years, ice melt is warranted. The actual percentage of runoff contribution within the catchment is related to the areal coverage of the cirque glaciers within the total

catchment of ~10% (Figure 1(b)) and is assumed to remain constant over the time period of 4 years. Input data for the model are daily values of precipitation and average temperature for the catchment.

Discharge data from the gauging station are used to calibrate and validate the model using split sample tests (e.g., Klemes, 1986). The results are compared to the hydrograph analyses and natural and artificial tracer data, thereby allowing to differentiate the various input ("recharge") components over time (in contrast to the other data that indicate discharge variations). Moreover, the model is then used to hypothetically remove/ignore the cirque glacier ice stores and explore potential changes in the runoff characteristics. In addition, the model parameters representing a relict rock glacier (Wagner et al., 2016) can be used to account for a hypothetical decay from an active to a relict rock glacier (a trading space-for-time approach accounting for changing watershed behaviour; Singh et al., 2011) and observe a potential change in storage-discharge characteristics.

3.4 | Glacier mass loss

The reduction in the areal extents of the two cirque glaciers within the rock glacier catchment was calculated for the time period 2006–2015 (Figure 1(b)) using the glacier inventories GI3 of Fischer et al. (2015) and GI4 of Buckel and Otto (2018). The corresponding ice volume loss was estimated based on a thickness-area scaling relation (e.g., Chen & Ohmura, 1990; discussed in Azócar & Brenning, 2010). Assuming a linear trend in volume loss for the 9 years between the two glacier extents, an estimated annual average ice loss was computed. Assuming further an ice density of ~900 kg/m^3, the water equivalent lost per year was estimated. This order of magnitude estimate is used as a plausibility check for the glacier ice meltwater contribution of the rainfall-runoff model as no direct information regarding runoff from the cirque glaciers is available.

4 | RESULTS AND INTERPRETATION

4.1 | Discharge components

Figure 4 depicts the updated hydrograph analysis of Wagner, Brodacz, et al. (2020), extended by an additional year of data. Master recession curves derived from single recessions to infer a theoretical recession curve over a long period of time indicate at least a fast-and a slow-flow component. Importantly, runoff at the rock glacier springs is still present in winter (base flow) with a discharge of a few l/s. The additional data strengthen the results of Wagner, Brodacz, et al. (2020), who related this base flow to the unfrozen base layer of the active rock glacier (Hausmann et al., 2012). In general, the variable discharge behaviour ranging from 6.5 L/s up to 718 L/s with a discharge ratio of 110 (Qmax/Qmin) is similar to the pattern observed at karst springs (e.g., Wagner, Brodacz, et al., 2020; Winkler et al., 2016).

The results of the artificial tracer tests indicate a fast-flow component exhibiting a mean residence time of around 9 h (Figure 5; 2015: 9:16 h; 2017: 8:41 h). When the tracer was injected into the glacial meltwater creek, this locally infiltrating meltwater significantly contributed to the fast-flow component. Peak flow velocities during the 2015 (recovery rate 45.8%) and 2017 (recovery rate 40.0%) tests were 0.061 and 0.047 m/s, respectively, while the mean flow velocity was 0.029 m/s during both tests.

The seasonal variations in discharge components are deciphered using natural tracers. EC measured at the gauging station ranges from 68 to 281 μS/cm, indicating an average fast-flow contribution of 42.6% (assuming a value of 20 μS/cm for event water EC) over the whole time period by applying a two-component mixing model and not further differentiating fast-flow derived from rainfall, snowmelt and / or ice melt (see Figure 6). The measured EC of glacial meltwater ranges from 1.2 to 4 μS/cm, while the measured EC of a single precipitation sample within the catchment is 42 μS/cm (sampling sites

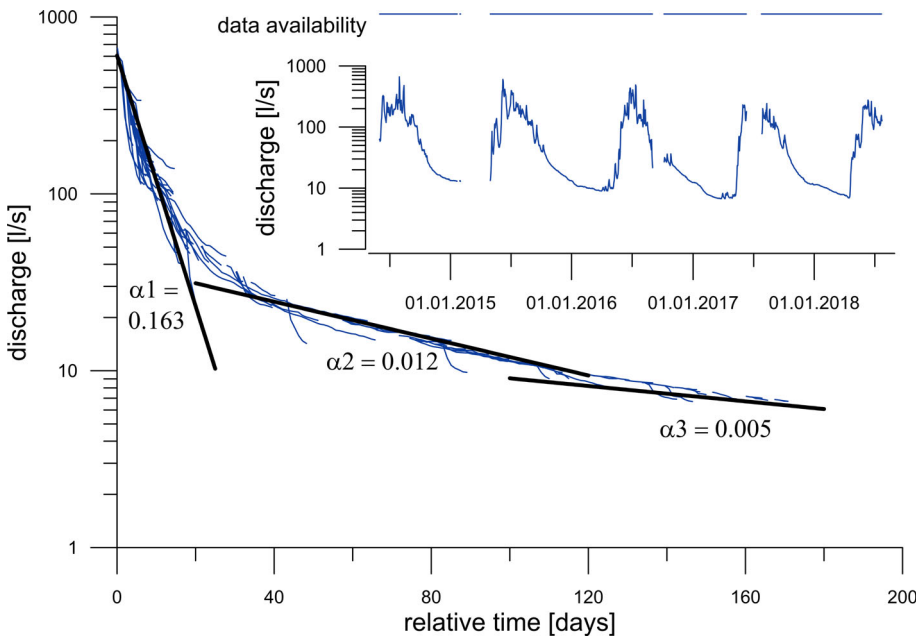

FIGURE 4 Master recession curve and the interpreted recession coefficients shown as straight lines in a semi-log plot and the spring hydrograph as an inset. Modified after Wagner, Brodacz, et al. (2020) and extended with more recent data (a time period in which also natural tracer data became available)

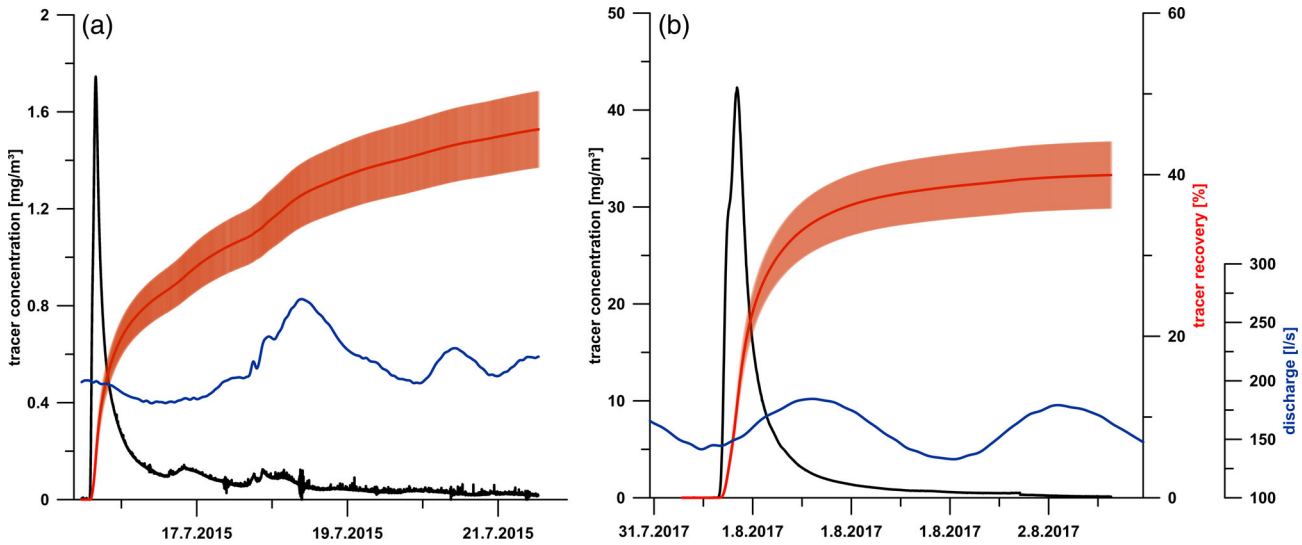

FIGURE 5 Artificial tracer breakthrough curve of (a) 2015 and (b) 2017 with a range of tracer recovery reflecting uncertainties in the runoff computation. Note the different scale of the tracer concentration for (a) and (b); tracer recovery and discharge are displayed at the same scale

indicated in Figure 1(b)). This value is unusually high for a pristine catchment. The event water end member of the two-component mixing model is therefore assigned an EC of 20 μS/cm, which would be an average of the values presented above but more importantly is similar to values used in alpine catchments by Wetzel (2003) and Winkler et al. (2016). The delayed groundwater EC is parametrized using the highest measured EC at the gauging station (281 μS/cm, measured at a discharge of 22 L/s on 5 November 2015). Presumably, even higher EC values would have been measured if the EC probe would not have fallen dry during the winter months characterized by very low discharge.

In general EC and discharge are inversely correlated (Figure 6). The overall variation in discharge components reflects the superposition of several regularly repeating patterns, exhibiting periods ranging from 1 day to 1 year (Heigert, 2018). Following the onset of snowmelt in spring, the fast-flow contribution increases until discharge reaches its maximum in early summer (Figure 6(a)). Its exact contribution is strongly dependent on local weather conditions, reflecting the variable snowmelt intensity in response to air temperature (note variability in both discharge and EC/fast-flow component during May in Figure 6(a)). Maximum discharge (several hundred l/s) is reached in early summer, indicating also the maximum level of storage within the rock glacier. At this time fast-flow accounts for up to 75% of the total discharge and is subject to pronounced diurnal variations (Figure 6(a),(b)). As summer progresses the overall discharge decreases and the fast-flow component reduces accordingly, resulting in a mean contribution of ~60% during the summer months. Prominent peaks after heavy rainfall on melting snow cover (early summer) and intense thunderstorms (late summer) are superimposed on this pattern, while peak magnitude decreases steadily during summer (Figure 6(a),(b)). Dry, warm summer periods induce pronounced diurnal variation in EC mirroring the diurnal discharge variations (Figure 6(b),(c)). Declining air temperatures strongly reduce discharge as well as fast-flow contribution and attenuate diurnal variations - temporarily during the summer months (Figure 6(a) around 23 June 2017) but persistently at the beginning of autumn (Figure 6(b) around 1 September 2017). After the first snowfall, spring flow steadily declines (~Sep.; Figure 6(b)) and the delayed flow contribution increases towards 100% (~Nov; see Figure 7 for snow dynamics) until the next snowmelt in early spring, occasionally intermitted by single peaks in response to warm rainfall events (Figures 2, 6(b)). No diurnal variations are observable during these periods of time.

Figure 6(c) depicts the periodic variation in discharge and natural tracers during a dry, warm summer period in early August 2017, following a heavy precipitation event in late July. The time lag between the diurnal air temperature maximum and peak discharge equals 16 h. Since snow was absent in the catchment, the periodicity is caused by ice melt responding to diurnal variation in radiation and air temperature. Note that EC and $\delta^{18}O$ are inversely correlated to discharge due to the dilution with ice meltwater exhibiting low EC (~2 μS/cm) compared to longer stored, delayed groundwater (281 μS/cm), confirmed by the corresponding variation in $\delta^{18}O$. However, differentiating permafrost ice melt from cirque glacier ice melt is not possible due to the lack of data concerning the former.

While the two-component mixing model indicates a mean fast-flow contribution of ~65% during the period depicted in Figure 6(c), plotting EC against $\delta^{18}O$ allows a more detailed analysis of the fast-flow component (Figure 6(d)). The observable hysteresis clearly indicates a dynamically changing composition of the fast-flow component (Harrington et al., 2018; Williams et al., 2006). The diurnal variation introduced by periodic dilution of groundwater with meltwater is superimposed on a general trend towards lower $\delta^{18}O$ values (Figure 6(c), (d)). This trend indicates a progressive shift from rainwater (around −8.05‰) towards ice meltwater (around −15.3‰) constituting the fast-flow component. Decreasing rainwater contributions correspond to continued runoff since the last heavy rainfall event on 29 July

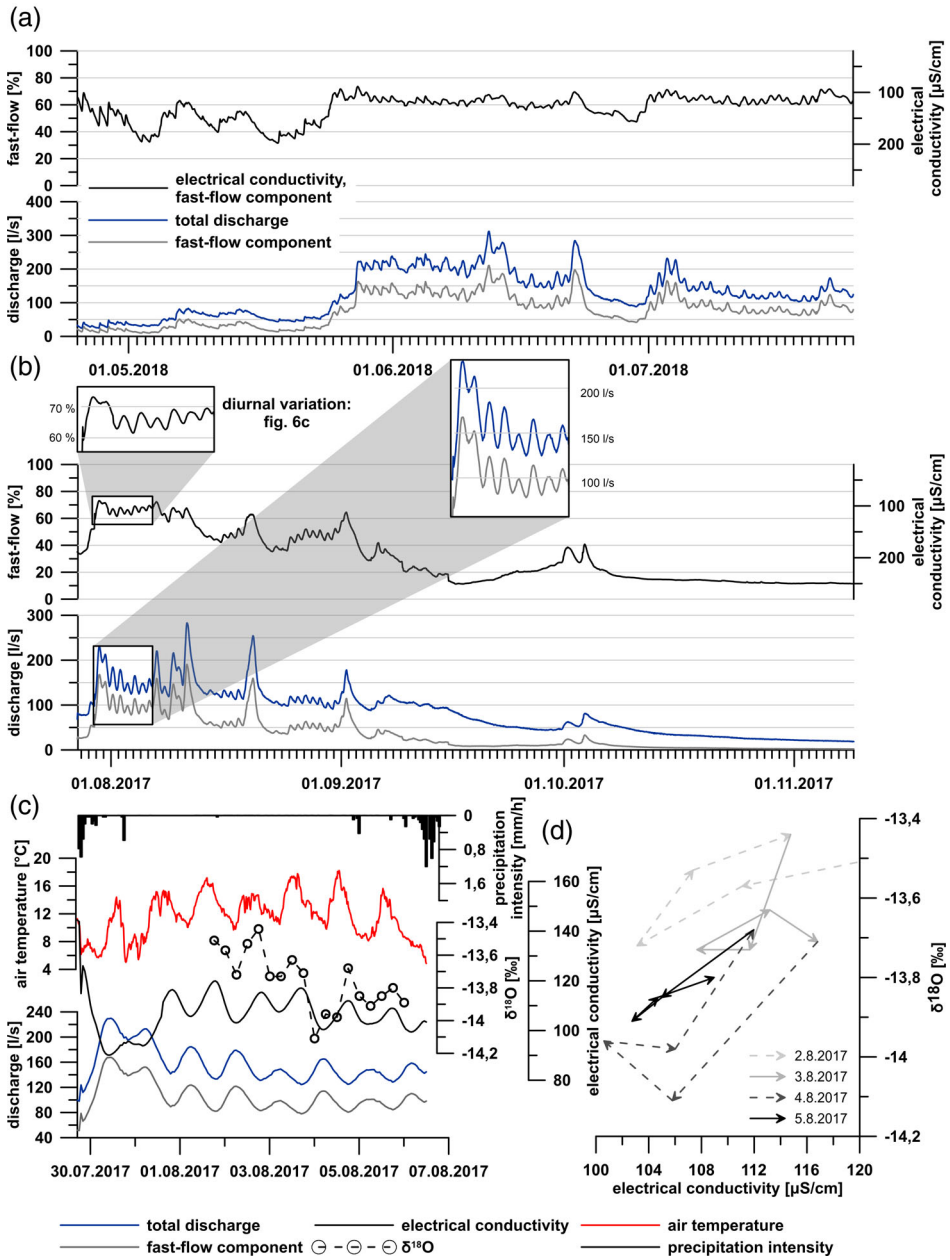

FIGURE 6 Natural tracer data. Runoff separation based on EC related to longer stored / higher mineralized groundwater. (a) Snowmelt period; (b) summer to autumn period with diurnal variations that are shown in more detail in (c) including air temperature, precipitation and isotopic data. (d) Observed hysteresis in EC versus isotopic data indicating dynamics in fast-flow components (ice melt, rainfall) versus delayed groundwater flow

2017. A minor rainfall event that occurred during the night from 4 August to 5 August 2017 (Figure 6(c)) immediately shifts the diurnal cycle towards higher $\delta^{18}O$ values on 5 August 2017 (Figure 6(d)). The simple two-component mixing model is merely a projection of the actual mixing process involving multiple sources as well as temporary storage within the catchment (see Section 4.2). Nonetheless, a high portion of fast-flow during these times, when rainfall events and ice melt coincide, becomes apparent.

4.2 | Recharge components / discharge pattern

Applying the lumped-parameter rainfall-runoff model yields satisfactorily results visually (Figure 7) as well as expressed in average Nash–Sutcliffe efficiency ($\bar{NSE}$) criteria (89.6%; Nash & Sutcliffe, 1970). $\bar{NSE}$ values using a split sample test (Klemes, 1986), where the model is calibrated on the first half of the available data set, validated on the second half and vice versa and compared to the complete data set are shown in Table 1 for calibration and validation periods. The model performs in a similar way as for the relict Schöneben rock glacier ($\bar{NSE}$ of 89.5%; Wagner et al., 2016). An average Nash–Sutcliffe efficiency ($\bar{NSE}$) criteria is computed using a combination of the classic Nash–Sutcliffe efficiency criterion (Nash & Sutcliffe, 1970) and the modified Nash–Sutcliffe criteria based on log-transformed and square root-transformed discharges (see Wagner et al., 2013, 2016). Also here, the physical relevance of model parameters is stressed (Mouelhi et al., 2006; Wagner et al., 2013, 2016). Table 2 shows the model parameter set from the best-fit model for the catchment of the active rock glacier Innere Ölgrube as well as the parameter set from the relict Schöneben rock glacier catchment (cf. Wagner et al., 2016).

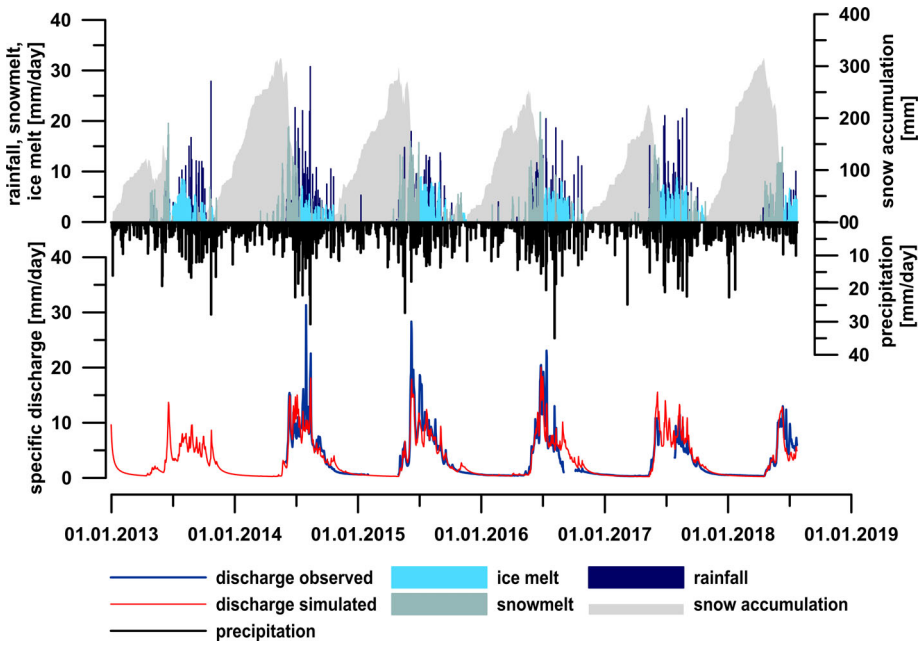

FIGURE 7 Observed and modelled discharge of the Innere Ölgrube spring catchment. Visual fit between observed and modelled discharge and related precipitation input data. Differentiation of rainfall, snowmelt and ice melt input as well as snow accumulation over the winter periods

TABLE 1 Model calibration efficiency criteria $\bar{NSE}$ [%] using a split sample test

$\bar{NSE}$ Efficiency criteria	Complete time series	First half of data set	Second half of data set
calibration on total time series	89,59	90,58	87,12
calibration on first half of data set	88,80	91,53	83,43
calibration on second half of data set	87,76	86,59	88,65

Comparable to the results of the relict Schöneben rock glacier catchment, a relatively large routing store (×3) is needed to achieve acceptable model fits. This is suggested to be related to the unfrozen base layer within the rock glacier, which was shown to exist by Hausmann et al. (2012) and interpreted to be the dominant shallow aquifer within the spring catchment (Wagner, Brodacz, et al., 2020). The production store (×1; or soil moisture accounting store) is even smaller than that of the Schöneben rock glacier catchment. Again, this relates physically

TABLE 2 Model parameter sets and model efficiency criteria of the rainfall-runoff model for the active Innere Ölgrube and the relict Schöneben rock glacier spring catchments; efficiency criteria are given for the whole time series. For more details on the relict Schöneben rock glacier, refer to Wagner et al. (2016)

		Active rock glacier	Relict rock glacier
		Innere Ölgrube	Schöneben
efficiency criteria [%]	$\bar{NSE}$	89,59	89,47
	$NSE\ Q$	84,17	89,50
	$NSE\ \sqrt{Q}$	91,05	90,10
	$NSE\log Q$	93,55	88,79
	WB	99,18	97,58
model parameters	x_1 [mm]	18,45	89,78
	x_2 [mm]	4,99	9,40
	x_3 [mm]	213,84	302,82
	x_4 [days]	1,27	1,15
	T_s [°C]	-0,47	1,05
	T_m [°C]	-0,44	4,10
	C_m [mm/°C]	1,88	3,32
	T_{im} [°C]	1,10	–
	C_{im} [mm/°C]	6,96	–

to the fact that the Innere Ölgrube catchment is basically a bare rock / debris field and evapotranspiration is limited. Interestingly, model parameters ×1 to ×4 are not very different from those of the relict Schöneben rock glacier catchment. These implications will be discussed in Section 5.

The rainfall-runoff model for the Innere Ölgrube rock glacier spring catchment allows a quantification of relative input derived from rainfall, snow- and ice melt (Figure 7). The corresponding input fractions for the observed period of time are 36.6%, 35.8% and 27.6%, respectively. It has to be noted, that ice melt is considered to be derived mainly from the melt of the cirque glaciers as indicated by artificial and natural tracer analyses (see discussion section). Berger et al. (2004) also reported about 30% of the rock glacier spring runoff to be related to the glacier meltwater supporting our findings.

4.3 | Glacier mass loss estimates from glacier inventories

Based on the two glacier inventories, a loss of 1.14×10^6 m^3 for the two cirque glaciers over the time period 2006–2015 was calculated, which is 0.13×10^6 m^3 on average per year. This is the same order of magnitude and about twice of what is "needed" in the rainfall-runoff model for the years 2015–2018; however, the areal extents of the cirque glaciers are even smaller by now and moreover the difference between ablation and actual melt needs to be considered. Sublimation is not considered here and therefore ablation estimates from the area-thickness relation will be higher than the glacier meltwater "input" estimated in the rainfall-runoff model. The data analysis allows an order of magnitude consistency check, but not more. Approximately 30% of the recharge are derived from meltwater of the cirque glaciers. When considering this rather significant contribution, a future glacier loss is supposed to have a significant impact on the runoff pattern.

5 | DISCUSSION

Despite the obvious difficulty of gathering data in high alpine catchments, the complementary information derived from natural and artificial tracer data and from a rainfall-runoff model (i.e., a water balance) allowed a thorough quantification of recharge and discharge components of the catchment of the active rock glacier Innere Ölgrube at present. Recharge components vary seasonally as well as diurnally, reflecting varying contributions from rainfall, snowmelt and ice melt. Discharge components are delayed to a certain extent due to the storage capabilities of the shallow aquifer within the rock glacier catchment (Wagner, Brodacz, et al., 2020), depending on the flow paths and saturation status of the groundwater body (Winkler et al., 2016, 2018).

The tracer velocities are in the range of reported values in active layers (Buchli et al., 2013; Krainer & Mostler, 2002; Tenthorey, 1992). The low recovery rate (< 50%) likely indicates that some of the tracer is lost to the deeper domains of the rock glacier (potentially the unfrozen base layer). The tracer is presumably stored there for a longer period of time, thereby preventing it from reaching the measurement device at a detectable concentration within the observation period. Yet, the fast recovery of at least 40% of the tracer clearly indicates a fast-flow component likely related to lateral flow on top of the permafrost table towards the rock glacier spring. This is also reflected in the hydrograph analysis. Concerning the delayed flow component related to the unfrozen sediment layer (subpermafrost flow) at the base of the rock glacier and potentially other fine sediments within the catchment (e.g., till deposits and moraines between the cirque glaciers and the rock glacier) EC and isotopic data was analysed.

Figure 8 depicts the seasonal variations in individual "recharge" and discharge component contributions. "Recharge" is inferred from the rainfall-runoff model (Figure 8(a)) and does not take the loss due to evapotranspiration into account, as this process is happening in the production store (Figure 3) where the different input components are already mixed and evapotranspiration is dependent on the saturation / water level within that store. The rainfall-runoff model estimates evapotranspiration to be ~21% of the total input, which is in good agreement with values in this area of Tyrol (17–22%) provided in the digital Hydrological Atlas of Austria (BMLFUW, 2007). Discharge is inferred from flow component analysis (Figure 8(b)), where higher-EC water is related to longer stored groundwater and low-EC water is related to fast-flow derived from snowmelt, ice melt or rainfall. The actual differentiation of fast-flow into rainfall, snowmelt and ice melt is not possible for that time frame (see Figure 6(c),(d) for a detailed analysis over a short period of time using isotopic data in addition to EC). The exact EC of event water entering the system was assumed to be 20 μS/cm (based on literature values). Considering a measured range of 5–40 μS/cm for event water (rainfall, snowmelt and/or ice melt), the total average fast-flow component estimated to be 42.6% would vary between 40.5% and 46.4%, depicting that uncertainties related to this input parameter are minor.

Combining the information of Figure 8(a) and (b) allows for an interesting interpretation. The delayed flow component (longer stored, higher-EC water within the aquifer; for example, Winkler et al., 2016, 2018) is the most important component during periods of little to no recharge (e.g., winter time; Wagner, Brodacz, et al., 2020). Snowmelt and (subordinately) rainfall are the dominant recharge components during early summer, rapidly increasing the fast-flow contribution to ~60%. In particular during dry summer periods and after snow has melted, ice (glacier or permafrost ice) runoff and delayed groundwater discharge become the relevant components. Separating delayed groundwater flow and ice meltwater due to the diurnal pattern of the melting process (related to variations in air temperature) is possible. The pronounced change in discharge pattern in early autumn observable in Figure 6(b) (reduced discharge and attenuated diurnal variations caused by declining air temperatures in early September) indicates the transition from the fast-flow dominated period (late April–August) to the delayed flow dominated period (September until onset of the snowmelt in April–early May). Some caution is required when interpreting relative discharge component contributions during

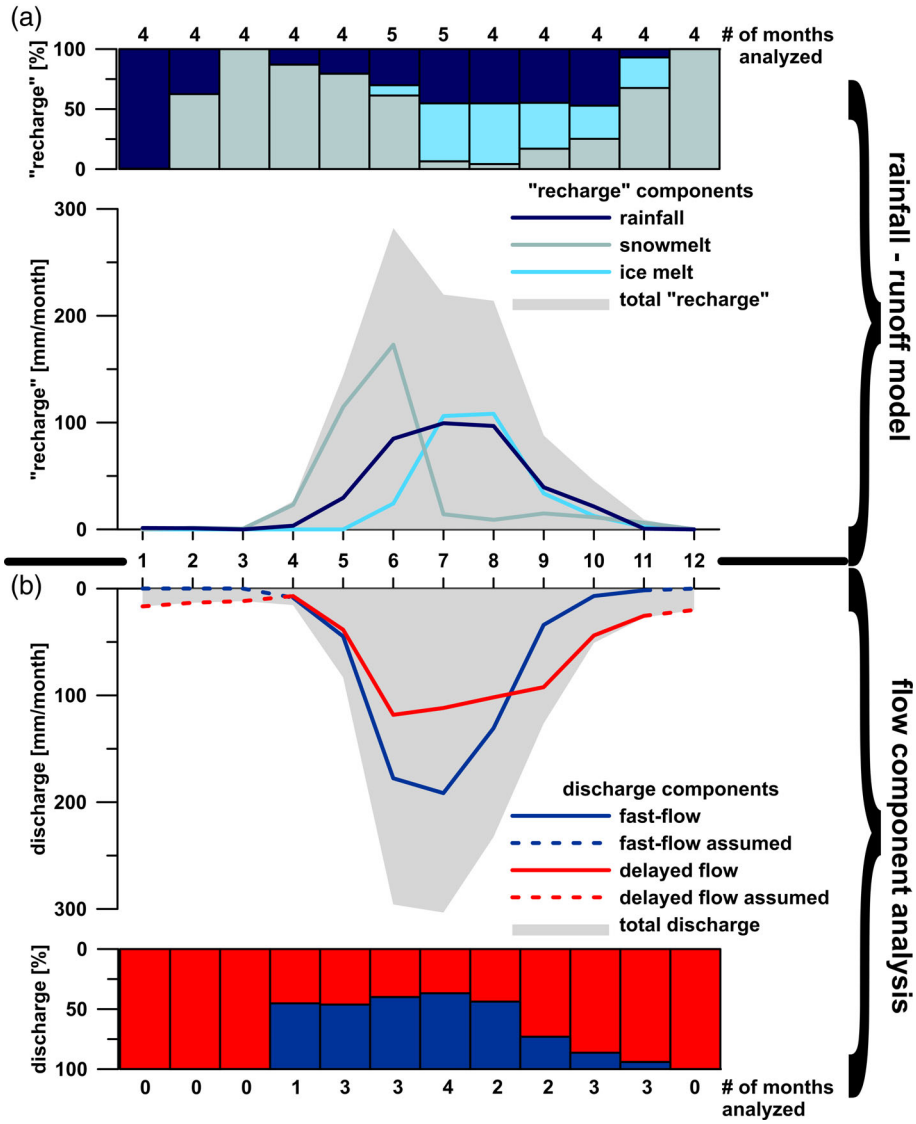

FIGURE 8 Monthly contribution of "recharge" (input into the rainfall-runoff model without considering potential loss due to evapotranspiration) and discharge components (based on flow component analysis); values normalized to catchment area. Shaded area indicates total flux. Dashed lines indicate assumed delayed flow/fast-flow contribution during periods of low discharge (no EC record available). Numbers next to bars indicate the number of months analysed (see Figure 2)

the onset of snowmelt in April (Figure 8), since the only available EC time series during that month starts on 25 April 2018. Thus, the delayed flow contribution during (early) April is likely underestimated in Figure 8.

To identify and quantify the main source of the ice meltwater potentially from permafrost ice melt or from the upper cirque glaciers is more complex. Natural and artificial tracer test results show that fast-flow components travel through the rock glacier within several hours. Ice-derived meltwater can be observed with a time lag in the order of ~16 h relative to air temperature indicated by EC and isotopic data (Figure 6(c)). This time lag in combination with the fast response due to event water suggests some distance of the meltwater source to the spring/rock glacier and favours the cirque glaciers as the main meltwater source. This is further substantiated by comparing the time lag to the artificial tracer test results: The linear distance between the lowermost point of the cirque glacier and the gauging station is approximately 1500 m, indicating an actual flow distance ≥1500 m. Typically, runoff from glaciers reaches a maximum a few hours after the peak in meltwater production (Cuffey & Paterson, 2010), thus the runoff peak at the glacier precedes the peak at the gauge by ≤16 h. Both estimates suggest that the water travels from the front of the glacier to the gauging station at a velocity ≥ 0.026 m/s. This is in good agreement with the artificial tracer test results yielding slightly higher linear velocities. Note also that melting rates at the cirque glaciers reflect diurnal variations in radiation, heat and vapour content of the adjacent air (Cuffey & Paterson, 2010). The coarse grained active layer covering the permafrost ice within the catchment protects it from radiation and induces a damped and retarded variation in temperature, decoupling it from external weather and climate conditions (Haeberli, 1985; Jones et al., 2019; Vonder Mühll, 1993; Wagner, Kainz, et al., 2019; Wagner, Pauritsch, et al., 2019). Accordingly, melting of permafrost ice is expected to follow changes in atmospheric conditions in a more damped and retarded fashion, suggesting cirque glacier melting to account for the observed diurnal variation in discharge and natural tracers.

The amount of ice melt is in the order of 30% of the annual recharge and will decrease and finally disappear in the future due to glacier melt. Thus, ignoring ice contribution from cirque glacier melt is hypothetical, but interesting at least. This can be assessed by using the calibrated rainfall-runoff model and assuming that ice melt from the cirque glaciers is absent due to potential future complete glacier melt (green line in Figure 9). This was simulated in a simplified manner by actually eliminating the (glacier) ice storage, keeping all the other parameters constant although disappearing glaciers might leave moraine sediments behind, which might increase the capacity of the routing store (×3). Increasing runoff during snowmelt periods does not change expectedly; however, the runoff in late summer indicates a certain reduction. Interestingly, base flow during winter months does not change significantly. This is an important finding that further supports that base flow is mainly derived from the unfrozen base layer of the rock glacier (and other fine-grained sediments in the catchment area [e.g., till deposits, moraines]; cf. Wagner, Brodacz, et al., 2020). In total, a runoff reduction of almost 30% is expected in this hypothetical scenario due to the disappearance of the cirque glaciers.

Another hypothetical scenario can be constructed by applying the model parameters of a relict rock glacier where the same model was already applied (Table 2; cf. Wagner et al., 2016) for the current setting of the active rock glacier. This trading space-for-time approach accounting for changing watershed behaviour under permafrost-free conditions (Singh et al., 2011) allows to speculate how progressing climate change might influence the discharge pattern, considering the associated uncertainties (purple line in Figure 9).

Changes are not substantial and only a slightly more buffered behaviour during storm events or snowmelt periods is visible compared to the scenario where only the ice melt from the glaciers is neglected. Interestingly, slightly slower recessions at the onset of winter periods are observable. This can be explained by a higher routing store x3 for the relict (Schöneben) rock glacier catchment than the active (Innere Ölgrube) rock glacier catchment. This might indicate an increase in storage capacities as permafrost thaw potentially leads to more available pore space in the shallow aquifer system (cf. Rogger et al., 2017). Nevertheless, in the case of the relict Schöneben rock glacier as well as for the active Innere Ölgrube rock glacier, both are known to have a rather fine-grained, unfrozen base layer that is 10–15 meters thick. These similarities might explain their rather similar behaviour, although one may speculate about a further increase in storage capacity within the Innere Ölgrube catchment as permafrost thaws eventually. This potential change is depicted by computing the master recession curves of the modelled runoff patterns for the "current" data, the hypothetical scenario of vanished cirque glaciers and the other hypothetical scenario of a relict rock glacier (Figure 10). The comparison to the observed data further indicates the good model fit in addition to the efficiency criteria and visual fit of the hydrographs presented before (and shown again in the inset). In addition, a dQ/dt versus Q analysis (e.g., Basso et al., 2015; Pauritsch et al., 2017) is provided as supplementary information (Figure S1) to depict that catchment hydrologic response is assured over the complete discharge range from very small to very high rates (cf. Basso et al., 2015). The similar master recession curves of the "current" data and the hypothetical one without the glacier ice melt is to be expected, as the actual internal (or model) structure did not change, but only a recharge component was "removed." The discharge pattern and consequently master recession curve of the hypothetically relict rock glacier catchment (using the parameter set of the relict Schöneben rock glacier; Wagner et al., 2016) indicates a slightly slower recession during winter periods as storage capabilities increase.

Uncertainties within the analysis can be divided into uncertainties of input variables (precipitation, air temperature), of the model structure and model parameters and finally uncertainties related to the two hypothetical scenarios of vanishing ice glaciers and the trading space-for-time approach.

The uncertainty related to input variables is similar to uncertainties in other alpine catchments and one reason why such parsimonious lumped parameter rainfall-runoff models are applied (e.g., Wagner et al., 2016). The difficulty of measuring precipitation, especially solid precipitation during windy conditions, is known (e.g., Sevruk et al., 2009). The input from glacier ice melt is also uncertain as no direct measurements were available. This is why the glacier inventories of two different time periods have been compared to provide an order of magnitude bandwidth.

An effort to reduce uncertainties in the model structure and model parameters has been taken by using an established model

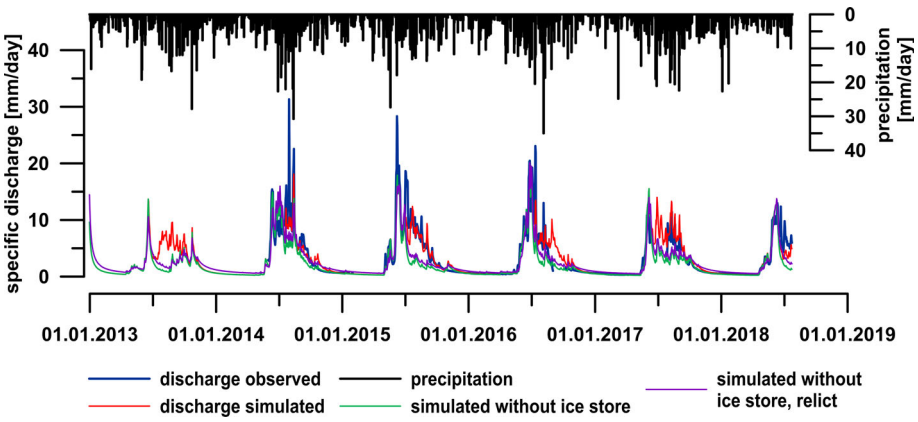

FIGURE 9 Observed discharge (dark blue line), modelled discharge (green line) without the input from the ice store, assuming cirque glaciers have vanished; and modelled discharge (purple line) without the input from the ice store and applying model parameters from the relict Schöneben rock glacier (Table 2; cf. Wagner et al., 2016); assuming the cirque glaciers as well as all the permafrost ice have vanished. Red line refers to the simulated runoff as in Figure 7

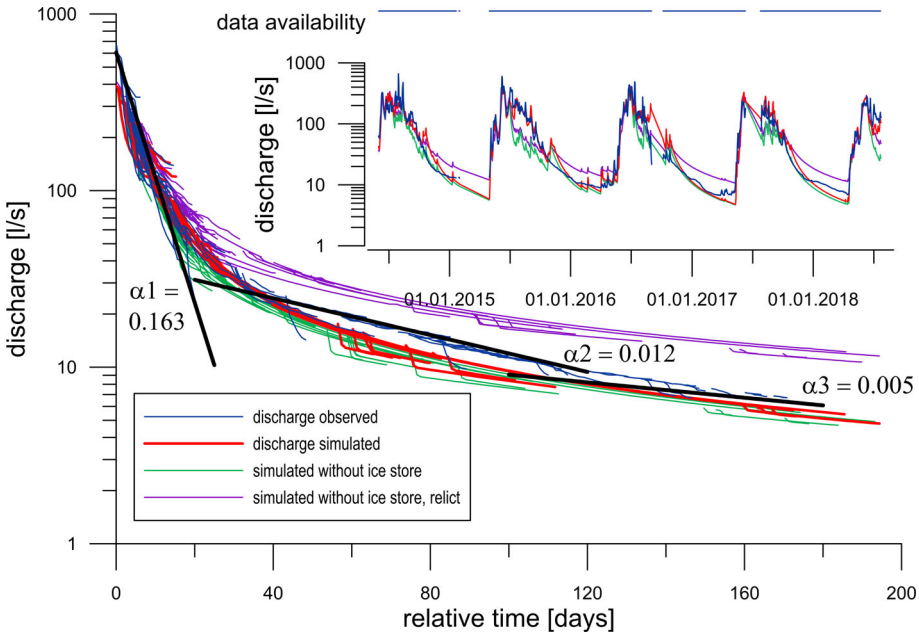

FIGURE 10 Master recession curves (MRC) of observed as well as simulated runoff; in addition, the simulated MRCs without the ice melt and the hypothetic scenario of a relict rock glacier in the (far?) future

structure and applying model efficiency criteria that are well established.

Uncertainties related to the two hypothetical scenarios are hard to quantify but obvious. Removing glacier ice melt from the model is interesting at least, but the model approach did not take any further changes into account that might occur due to glacier ice loss. Potential increase in, for example the routing store (×3) can be discussed, but is beyond the scope of this work. No active rock glacier spring catchment without a cirque glacier in its catchment area has been modelled so far. The uncertainties related to the trading space-for-time approach are likely even larger, as there is only a single other rock glacier (a relict one) for which calibrated model parameters are available. This further highlights the need of long-term monitoring data.

What remains to be identified is the actual contribution of permafrost ice melt at present and future changes in the runoff pattern due to this additional water in the short term and potential increases in the storage capacity in the long term when the permafrost ice will melt completely. The trading space-for-time approach presented herein does suggest a slight difference in runoff patterns and supports what was suggested by Rogger et al. (2017): Runoff might be dampened slightly and storage capacities might increase to some extent. However, further research addressing this particular case and ideally monitoring rock glacier catchments without the influence of cirque glaciers within their catchment is needed. Colombo et al. (2018) suggest establishing baselines for future monitoring related to downstream water quality (and quantity) as solute export from deteriorating rock glaciers might provide valuable information.

In alpine catchments, rock glaciers should be seen as hydro(geo)logically (and geomorphologically) conservative systems (Giardino et al., 1992) that become increasingly important as ice glaciers will continue to vanish. For a recent assessment of potential changes in the European mountain cryosphere until the end of the 21st century, see Beniston et al. (2018). There, improvements in understanding changes in re- as well as discharge in high-alpine areas are warranted. The here gathered information and developed understanding of a high-alpine spring catchment that drains an active rock glacier and two cirque glaciers is of importance and should be extended by including downstream observations (cf. Wagner et al., 2016). Another open question remains the actual contribution of permafrost ice melt relative to the glacier ice melt and becomes increasingly important with regard to climate change and a likely further warming trend. A recent review about potential ecosystem shifts in alpine streams highlights the importance of a better understanding of permafrost/rock glacier thaw (Brighenti et al., 2019). Therefore, long-term monitoring of such high-alpine catchments (and streams further downstream) is essential.

6 | CONCLUSIONS

Applying a number of "standard" hydrogeological tools in a high alpine catchment allows the differentiation and the quantification of multiple recharge sources for and subsequently fast and delayed discharge from a shallow groundwater aquifer, that is an active rock glacier. Faster flow through the system is accomplished by suprapermafrost flowpaths, whereas slower flow by subpermafrost flowpaths; although intermediate flow paths are to be expected and indicate the complex internal structure of these landforms. Delayed groundwater flow contribution does play an important role in rock glacier spring discharge, especially during the winter months or periods of little recharge. Ice melt contribution from cirque glaciers within the catchment of the rock glacier spring mask the potential – but likely still negligible – influence of permafrost ice melt during snow-free periods. A future scenario with vanished cirque glaciers, diminishing amounts of permafrost ice within the rock glacier and thereby increasing storage capacity of the shallow groundwater store within the rock glacier might

suggest an increasing importance of these (ice-) debris accumulations in shaping the runoff pattern of alpine catchments.

The storage-discharge characteristics of the investigated active rock glacier catchment is an example of a shallow groundwater aquifer in alpine catchments that ought to be considered when analysing (future) river runoff characteristics in alpine catchments as these provide retarded runoff during periods with little to no recharge. The provided steady baseflow and delayed release of water within such an alpine catchment is crucial to understand and critical to sustain ecological diversity in the light of climate change.

ACKNOWLEDGEMENTS

This work was co-funded by the Austrian Federal Ministry of Agriculture, Regions and Tourism (former Federal Ministry of Sustainability and Tourism) and the Federal States of Vorarlberg, Tyrol, Salzburg, Styria and Carinthia within the DaFNE projects RGHeavyMetal (Nr. 101093) and RG-AlpCatch (Nr. 101561). Digital elevation models were provided by the GIS Service of the Federal Government of Tyrol. We acknowledge the very constructive suggestions by Masaki Hayashi, an anonymous reviewer and the editor Gianluca Botter that greatly improved the paper.

DATA AVAILABILITY STATEMENT

Data available on request from the authors.

ORCID

Thomas Wagner https://orcid.org/0000-0001-9149-0305

REFERENCES

Arenson, L.U., Hauck, C., Hilbich, C., Seward, L., Yamato, Y., & Springman, S. (2010). Sub-surface Heterogeneities in the Murtèl – Corvatsch Rock Glacier, Switzerland. In: Canadian Geotechnical Society (eds.): Proceedings of the joint 63rd Canadian Geotechnical Conference and the 6th Canadian Permafrost Conference. Calgary, Alberta, S. 1494–1500.

Azócar, G. F., & Brenning, A. (2010). Hydrological and geomorphological significance of rock glaciers in the dry Andes, Chile (27°–33°S). *Permafrost and Periglacial Processes*, *21*(1), 42–53. https://doi.org/10.1002/ppp.669

Barsch, D. (1996). Rockglaciers: Indicators for the present and former geoecology in high mountain environments. In *Springer Series in Physical Environment* (Vol. 16). Springer.

Basso, S., Schirmer, M., & Botter, G. (2015). On the emergence of heavy-tailed streamflow distributions. *Advances in Water Resources*, *82*, 98–105. https://doi.org/10.1016/j.advwatres.2015.04.013

Beniston, M., Farinotti, D., Stoffel, M., Andreassen, L. M., Coppola, E., Eckert, N., Fantini, A., Giacona, F., Hauck, C., Huss, M., Huwald, H., Lehning, M., López-Moreno, J.-I., Magnusson, J., Marty, C., Morán-Tejéda, E., Morin, S., Naaim, M., Provenzale, A., … Vincent, C. (2018). The European mountain cryosphere: A review of its current state, trends, and future challenges. *The Cryosphere*, *12*, 759–794. https://doi.org/10.5194/tc-12-759-2018

Berger, J., Krainer, K., & Mostler, W. (2004). Dynamics of an active rock glacier (Ötztal Alps, Austria). *Quaternary Research*, *62*(3), 233–242. https://doi.org/10.1016/j.yqres.2004.07.002

Berthling, I. (2011). Beyond confusion: Rock glaciers as cryo-conditioned landforms. *Geomorphology*, *131*, 98–106. https://doi.org/10.1016/j.geomorph.2011.05.002

BMLFUW (Ed.). (2007). *Hydrologischer atlas Österreichs [hydrological atlas of Austria]. 3*. Lieferung. Bundesministerium für Land- und Frstwirtschaft. isbn:3-85437-250-7.

Brighenti, S., Tolotti, M., Bruno, M. C., Warthon, G., Pusch, M. T., & Bertoldi, W. (2019). Ecosystem shifts in alpine streams under glacier retreat and rock glacier thaw: A review. *Science of the Total Environment*, *675*, 542–559. https://doi.org/10.1016/j.scitotenv.2019.04.221

Buchli, T., Merz, K., Zhou, X., Kinzelbach, W., & Springman, S. (2013). Characterization and monitoring of the Fuggwanghorn rock glacier, Turtmann Valley, Switzerland: Results from 2010 to 2012. *Vadose Zone Journal*, *12*(1), 1–15. https://doi.org/10.2136/vzj2012.0067

Buckel, J., & Otto, J.-C. (2018). The Austrian glacier inventory GI 4 (2015) in ArcGis (shapefile) format. Pangaea, PANGAEA supplement to: Buckel, Johannes; Otto, Jan-Christoph; Prasicek, Günther; & Keuschnig, Markus (2018): Glacial lakes in Austria - Distribution and formation since the Little Ice Age. *Global and Planetary Change*, *164*, 39–51. https://doi.org/10.1594/PANGAEA.887415

Chen, J., & Ohmura, A. (1990). Estimation of Alpine glacier water resources and their change since the 1870s. In H. Lang & A. Musy (Eds.), *Hydrology in Mountainous Regions, I – Hydrological Measurements; the Water Cycle, Proceedings of two Lausanne Symposia, August 1990* (Vol. 193, pp. 127–135). IAHS Press.

Colombo, N., Salerno, F., Gruber, S., Freppaz, M., Williams, M., Fratianni, S., & Giardino, M. (2018). Review: Impacts of permafrost degradation on inorganic chemistry of surface fresh water. *Global and Planetary Change*, *162*, 69–83. https://doi.org/10.1016/j.gloplacha.2017.11.017

Cuffey, K. M., & Paterson, W. S. B. (2010). *The physics of glaciers* (4th ed.). Elsevier Butterworth Heinemann.

Fischer, A., Seiser, B., Stocker-Waldhuber, M., Mitterer, C., & Abermann, J. (2015). In: Fischer, A. (Ed.), The Austrian Glacier Inventories GI 1 (1969), GI 2 (1998), GI 3 (2006), and GI LIA in ArcGIS (Shapefile) Format. PANGAEA; Supplement to: Fischer, Andrea; Seiser, Bernd; Stocker-Waldhuber, Martin; Mitterer, Christian; & Abermann, Jakob (2015): Tracing glacier changes in Austria from the Little Ice Age to the present using a lidar-based high-resolution glacier inventory in Austria. https://doi.org/10.1594/PANGAEA.844988.

Giardino, J. R., Vitek, J. D., & Demorett, J. L. (1992). A model of water movement in rock glaciers and associated water characteristics. In J. C. Dixon & A. D. Abrahams (Eds.), *Periglacial geomorphology* (pp. 159–184). Wiley.

Groh, T., & Blöthe, J. H. (2019). Rock glacier kinematics in the Kaunertal, Ötztal Alps, Austria. *Geosciences*, *9*, 373. https://doi.org/10.3390/geosciences9090373

Haeberli, W. (1985). Creep of mountain permafrost. Internal structure and flow of alpine rock glaciers. Mitteilungen der Versuchsanstalt für Wasserbau, Hydrologie und Glaziologie der ETH Zürich, 77. Eidgenössische Technische Hochschule, Zürich.

Harrington, J. S., Mozil, A., Hayashi, M., & Bentley, L. R. (2018). Groundwater flow and storage processes in an inactive rock glacier. *Hydrological Processes*, *32*, 3070–3088. https://doi.org/10.1002/hyp.13248

Hausmann, H., Krainer, K., Brückl, E., & Mostler, W. (2007). Internal structure and ice content of Reichenkar rock glacier (Stubai Alps, Austria) assessed by geophysical investigations. *Permafrost and Periglacial Processes*, *18*, 351–367. https://doi.org/10.1002/ppp.601

Hausmann, H., Krainer, K., Brückl, E., & Ullrich, C. (2012). Internal structure, ice content and dynamics of Ölgrube and Kaiserberg rock glaciers (Ötztal Alps, Austria) determined from geophysical surveys. *Austrian Journal of Earth Sciences*, *105*(2), 12–31.

Hayashi, M. (2020). Alpine hydrogeology: The critical role of groundwater in sourcing the headwaters of the world. *Groundwater*, *58*(4), 498–510. https://doi.org/10.1111/gwat.12965

Heigert, K. (2018). Speicherverhalten und Abflussdynamik aktiver Blockgletscher am Beispiel "Ölgrube Süd," Kaunertal [storage and

discharge dynamics of active rock glaciers, example "Ölgrube Süd," Kaunertal valley]. *Beiträge zur Hydrogeolgie*, *62*, 33–42.

Hoinkes, G., & Thöni, M. (1993). Evolution of the Ötztal-Stubai, Scarlcampo and Ulten basement units. In J. F. von Raumer & F. Neubauer (Eds.), *Pre-Mesozoic geology in the Alps* (pp. 485–494). Springer.

Jones, D. B., Harrison, S., Anderson, K., Selley, H. L., Wood, J. L., & Betts, R. A. (2018). The distribution and hydrological significance of rock glaciers in the Nepalese Himalaya. *Global and Planetary Change*, *160*, 123–142. https://doi.org/10.1016/j.gloplacha.2017.11.005

Jones, D. B., Harrison, S., Anderson, K., & Whalley, W. B. (2019). Rock glaciers and mountain hydrology. A review. *Earth-Science Reviews*, *193*, 66–90. https://doi.org/10.1016/j.earscirev.2019.04.001

Kaminsky, E., Plan, L., Wagner, T., Funk, B., & Oberender, P. (2021). Flow dynamics in a vadose shaft – A case study from the Hochschwab karst massif (northern calcareous Alps, Austria). *International Journal of Speleology*, *50*(2), 157–172. https://doi.org/10.5038/1827-806X.50.2.2375

Klemes, V. (1986). Operational testing of hydrological simulation models. *Hydrological Sciences*, *31*(1), 13–24. https://doi.org/10.1080/02626668609491024

Krainer, K., & Mostler, W. (2002). Hydrogeology of active rock glaciers: Examples from the Austrian Alps. *Arctic, Antarctic and Alpine Research*, *34*(2), 142–149. https://doi.org/10.1080/15230430.2002.12003478

Krainer, K., & Mostler, W. (2006). Flow velocities of active rock glaciers in the Austrian Alps. *Geografiska Annaler: Series A, Physical Geography*, *88*, 267–280. https://doi.org/10.1111/j.0435-3676.2006.00300.x

Krainer, K., Mostler, W., & Spötl, C. (2007). Discharge from active rock glaciers, Austrian Alps; a stable isotope approach. *Austrian Journal of Earth Sciences*, *100*, 102–112.

Krainer, K., Bressan, D., Dietre, B., Haas, J. N., Hajdas, I., Lang, K., Mair, V., Nickus, U., Reidl, D., Thies, H., & Tonidandel, D. (2015). A 10,300-year-old permafrost core from the active rock glacier Lazaun, southern Ötztal Alps (South Tyrol, northern Italy). *Quaternary Research*, *83*(2), 324–335. https://doi.org/10.1016/j.yqres.2014.12.005

Kreft, A., & Zuber, A. (1978). On the physical meaning of the dispersion equation and its solutions for different initial and boundary conditions. *Chemical Engineering Science*, *33*(11), 1471–1480. https://doi.org/10.1016/0009-2509

Kuhn, M., Kuhn, M., Dreiseitl, E., & Emprechtinger, M. (2013). Temperatur und Niederschlag an der Wetterstation Obergurgl, 1953-2011. In E. M. Koch & B. Erschbamer (Eds.), *Klima, Wetter, Gletscher im Wandel* (pp. 11–30). Innsbruck University Press. isbn:978-3-902811-89.

Maillet, E. (1905). *Essais d'hydraulique souterraine et fluviale*. Librairie Scientifique A.

Majone, B., Bertagnoli, A., & Bellin, A. (2010). A non-linear runoff generation model in small alpine catchments. *Journal of Hydrology*, *385*, 300–312. https://doi.org/10.1016/j.jhydrol.2010.02.033

Mouelhi, S., Michel, C., Perrin, C., & Andréassian, V. (2006). Stepwise development of a two-parameter monthly water balance model. *Journal of Hydrology*, *318*, 200–214. https://doi.org/10.1016/j.jhydrol.2005.06.014

Nash, J. E., & Sutcliffe, J. V. (1970). River flow forecasting through conceptual models. Part I – A discussion of principles. *Journal of Hydrology*, *10*(3), 282–290. https://doi.org/10.1016/0022-1694

Nepal, S., Chen, J., Penton, D. J., Neumann, L. E., Zheng, H., & Wahid, S. (2017). Spatial GR4J conceptualization of the Tamor glaciated alpine catchment in eastern Nepal: Evaluation of GR4JSG against streamflow and MODIS snow extent. *Hydrological Processes*, *31*, 51–68. https://doi.org/10.1002/hyp.10962

Oudin, L., Hervieu, F., Michel, C., Perrin, C., Andréassian, V., Anctil, F., & Loumagne, C. (2005). Which potential evapotranspiration input for a lumped rainfall-runoff model? Part 2 – Towards a simple and efficient potential evapotranspiration model for rainfall-runoff modeling. *Journal of Hydrology*, *303*, 290–306. https://doi.org/10.1016/j.hydrol.2004.08.026

Pauritsch, M., Birk, S., Wagner, T., Hergarten, S., & Winkler, G. (2015). Analytical approximations of discharge recessions for steeply sloping aquifers in alpine catchments. *Water Resources Research*, *51*, 8729–8740. https://doi.org/10.1002/2015WR017749

Pauritsch, M., Wagner, T., Winkler, G., & Birk, S. (2017). Investigating groundwater flow components in an alpine relict rock glacier (Austria) using a numerical model. *Hydrogeology Journal*, *25*, 371–383. https://doi.org/10.1007/s10040-016-1484-x

Perrin, C., Michel, C. & Andréassian, V. (2003). Improvement of a parsimonious model for streamflow simulation. *Journal of Hydrology*, *279*, 275-289. https://doi.org/10.1016/S0022-1694%2803%2900225-7

Posavec, K., Giacopetti, M., Materazzi, M., & Birk, S. (2017). Method and excel VBA algorithm for modeling master recession curve using trigonometry approach. *Groundwater*, *55*(6), 891–898. https://doi.org/10.1111/gwat.12549

Rogger, M., Chirico, G. B., Hausmann, H., Krainer, K., Brückl, E., Stadler, P., & Blöschl, G. (2017). Impact of mountain permafrost on flow path and runoff response in a high alpine catchment. *Water Resources Research*, *53*, 1288–1308. https://doi.org/10.1002/2016WR019341

Schnegg, P.-A. (2002). An inexpensive field fluorometer for hydrogeological tracer tests with three tracers and turbidity measurement. XXXII IAH & ALHSUD Congress Groundwater and Human Development. Balkema, Mar del Plata, Argentina, 1484–1488.

Sevruk, B., Ondrás, M., & Chvíla, B. (2009). The WMO precipitation measurement intercomparisons. *Atmospheric Research*, *92*, 376–380. https://doi.org/10.1016/j.atmosres.2009.01.016

Shannon, S., Smith, R., Wiltshire, A., Payne, T., Huss, M., Betts, R., Caesar, J., Koutroulis, A., Jones, D., & Harrison, S. (2019). Global glacier volume projections under high-end climate change scenarios. *The Cryosphere*, *13*, 325–350. https://doi.org/10.5194/tc-13-325-2019

Singh, R., Wagener, T., van Werkhoven, K., Mann, M. E., & Crane, R. (2011). A trading space-for-time approach to probabilistic continuous streamflow predictions in a changing climate – Accounting for changing watershed behavior. *Hydrology and Earth System Sciences*, *15*, 3591–3603. https://doi.org/10.5194/hess-15-3591-2011

Tenthorey, G. (1992). Perennial névés and the hydrology of rock glaciers. *Permafrost and Periglacial Processes*, *3*(3), 247–252. https://doi.org/10.1002/ppp.3430030313

Vonder Mühll, D. S. (1993). Geophysikalische Untersuchungen im permafrost des Oberengadins [geophysical investigations of permafrost in the upper Engadin]. [doctoral dissertation] Eidgenössische Technische Hochschule, Zürich.

Wagner, T., Mayaud, C., Benischke, R., & Birk, S. (2013). Ein besseres Verständnis des Lurbach-Karstsystems durch ein konzeptionelles Niederschlags-Abfluss-Modell [A better understanding oft he Lurbach karst system via a conceptional rainfall-runoff model]. *Grundwasser*, *18*, 225–235. https://doi.org/10.1007/s00767-013-0234-4

Wagner, T., Pauritsch, M., & Winkler, G. (2016). Impact of relict rock glaciers on spring and stream flow of alpine watersheds: Examples of the Niedere Tauern range, eastern Alps (Austria). *Austrian Journal of Earth Sciences*, *109*(1), 84–98. https://doi.org/10.17738/ajes.2016.0006

Wagner, T., Kainz, S., Wedenig, M., Pleschberger, R., Krainer, K., Kellerer-Pirklbauer, A., Ribis, M., Hergarten, S., & Winkler, G. (2019). Wasserwirtschaftiche Aspekte von Blockgletschern in Kristallingebieten der Ostalpen – Speicherverhalten, Abflussdynamik und Hydrochemie mit Schwerpunkt Schwermetallbelastungen (RGHeavyMetal) – Endbericht. Final report, 158. https://www.bmnt.gv.at/wasser/wasserqualitaet/RG-HeavyMetal.html

Wagner, T., Pauritsch, M., Mayaud, C., Kellerer-Pirklbauer, A., Thalheim, F., & Winkler, G. (2019). Controlling factors of microclimate in blocky surface layers of two nearby relict rock glaciers (Niedere Tauern range, Austria). *Geografiska Annaler: Series A, Physical Geography*, *101*(4), 310–333. https://doi.org/10.1080/04353676.2019.1670950

Wagner, T., Brodacz, A., Krainer, K., & Winkler, G. (2020). Active rock glaciers as shallow groundwater reservoirs, Austrian Alps. *Grundwasser*, *25*, 215–230. https://doi.org/10.1007/s00767-020-00455-x

Wagner, T., Pleschberger, R., Kainz, S., Ribis, M., Kellerer-Pirklbauer, A., Krainer, K., Philippitsch, R., & Winkler, G. (2020). The first consistent inventory of rock glaciers and their hydrological catchments of the Austrian Alps. *Austrian Journal of Earth Sciences*, *113*(1), 1–23. https://doi.org/10.17738/ajes.2020.0001

Wagner, T., Ribis, M., Kellerer-Pirklbauer, A., Krainer, K., & Winkler, G. (2020). The Austrian rock glacier inventory RGI_1 and the related rock glacier catchment inventory RGCI_1 in ArcGis (shapefile) format. *PANGAEA*. https://doi.org/10.1594/PANGAEA.921629

Wetzel, K.-F. (2003). Runoff production processes in small alpine catchments within the unconsolidated Pleistocene sediments of the Lainbach area (upper Bavaria). *Hydrological Processes*, *17*, 2463–2483. https://doi.org/10.1002/hyp.1254

Williams, M. W., Knauf, M., Caine, N., Liu, F., & Verplanck, P. L. (2006). Geochemistry and source waters of rock glacier outflow, Colorado front range. *Permafrost and Periglacial Processes*, *17*, 13–33. https://doi.org/10.1002/ppp.535

Winkler, G., Wagner, T., Pauritsch, M., Birk, S., Kellerer-Pirklbauer, A., Benischke, R., Leis, A., Morawetz, R., Schreilechner, M. G., & Hergarten, S. (2016). Identification and assessment of groundwater flow and storage components of the relict Schöneben rock glacier, Niedere Tauern range, eastern Alps (Austria). *Hydrogeology Journal*, *24*, 937–953. https://doi.org/10.1007/s10040-015-1348-9

Winkler, G., Wagner, T., Krainer, K., Ribis, M., & Hergarten, S. (2018). Hydrogeology of rock glaciers – Storage capacity and drainage dynamics – An overview. In V. G. Sychev & L. Mueller (Eds.), *Novel methods and results of landscape research in Europe, Central Asia and Siberia* (Vol. II/71, pp. 329–334). Moscow: Pryanishnikov Institute of Agrochemistry.

Zenklusen Mutter, E., & Phillips, M. (2012). Thermal evidence of recent talik formation in Ritigraben rock glacier: Swiss Alps. In K. M. Hinkel (Ed.), *Resources and risks of permafrost areas in a changing world. Proceedings. Vol. 1: international contributions* (pp. 479–483). The Northern Publisher.

Zurawek, R. (2002). Internal structure of a relict rock glacier, Sleza massif, Southwest Poland. *Permafrost and Periglacial Processes*, *13*, 29–42. https://doi.org/10.1002/ppp.403

SUPPORTING INFORMATION

Additional supporting information may be found online in the Supporting Information section at the end of this article.

How to cite this article: Wagner, T., Kainz, S., Krainer, K., & Winkler, G. (2021). Storage-discharge characteristics of an active rock glacier catchment in the Innere Ölgrube, Austrian Alps. *Hydrological Processes*, *35*(5), e14210. https://doi.org/10.1002/hyp.14210